In silico anti-viral assessment of phytoconstituents in a traditional (Siddha Medicine) polyherbal formulation — Targeting Mpro and pan-coronavirus post-fusion Spike protein

Sumit Kumar Mandal [a], MD Muzaffar-Ur Rehman [b], Ashish Katyal [a], Kanishk Rajvanshi [a], Manoj Kannan [a, c], Mohit Garg [d], Sankaranarayanan Murugesan [b], P.R. Deepa [a, *]

[a] Department of Biological Sciences, Birla Institute of Technology & Science (BITS Pilani), Pilani Campus, Pilani, 333031, Rajasthan, India
[b] Medicinal Chemistry Research Laboratory, Department of Pharmacy, Birla Institute of Technology and Science Pilani, Pilani Campus, Pilani, 333031, Rajasthan, India
[c] Plaksha University, SAS Nagar, Mohali, 140306, Punjab, India
[d] Department of Chemical Engineering, Birla Institute of Technology and Science Pilani, Pilani Campus, Pilani, 333031, Rajasthan, India

ARTICLE INFO

ABSTRACT

Background and aim: Novel nature of the viral pathogen SARS-CoV-2 and the absence of standard drugs for treatment, have been a major challenge to combat this deadly infection. Natural products offer safe and effective remedy, for which traditional ethnic medicine can provide leads. An indigenous poly-herbal formulation, Kabasura Kudineer from Siddha system of medicine was evaluated here using a combination of computational approaches, to identify potential inhibitors against two anti-SARS-CoV-2 targets — post-fusion Spike protein (structural protein) and main protease (Mpro, non-structural protein).
Experimental procedure: We docked 32 phytochemicals from the poly-herbal formulation against viral post-fusion Spike glycoprotein and Mpro followed by molecular dynamics using Schrodinger software. Drug-likeness analysis was performed using machine learning (ML) approach and pkCSM.
Results: The binding affinity of the phytochemicals in Kabasura Kudineer revealed the following top-five bioactives: Quercetin > Luteolin > Chrysoeriol > 5-Hydroxy-7,8-Dimethoxyflavone > Scutellarein against Mpro target, and Gallic acid > Piperlonguminine > Chrysoeriol > Elemol > Piperine against post-fusion Spike protein target. Quercetin and Gallic acid exhibited binding stability in complexation with their respective viral-targets and favourable free energy change as revealed by the molecular dynamics simulations and MM-PBSA analysis. *In silico* predicted pharmacokinetic profiling of these ligands revealed appropriate drug-likeness properties.
Conclusion: These outcomes provide: (a) potential mechanism for the anti-viral efficacy of the indigenous Siddha formulation, targeting Mpro and post-fusion Spike protein (b) top bioactive lead-molecules that may be developed as natural product-based anti-viral pharmacotherapy and their pleiotropic protective effects may be leveraged to manage co-morbidities associated with COVID-19.

Taxonomy (classification by EVISE)

Disease health condition: COVID-19 viral respiratory infection.
Experimental approach: *in silico* technique; natural products.

1. Introduction

The COVID-19 pandemic was a wake-up call that prompted an unprecedented and urgent need to have a multi-pronged public health management approach, to deal with an infection (and its complications) which impacted human lives across the world, with

* Corresponding author.
E-mail addresses: p20190001@pilani.bits-pilani.ac.in (S.K. Mandal), p20210457@pilani.bits-pilani.ac.in (M.M.-U. Rehman), p20170101@pilani.bits-pilani.ac.in (A. Katyal), f2016188@pilani.bits-pilani.ac.in (K. Rajvanshi), manoj.kannan@plaksha.edu.in (M. Kannan), mohit.garg@pilani.bits-pilani.ac.in (M. Garg), murugesan@pilani.bits-pilani.ac.in (S. Murugesan), deepa@pilani.bits-pilani.ac.in (P.R. Deepa).

List of abbreviations

SARS-CoV-2	Severe Acute Respiratory Syndrome Coronavirus 2
WHO	World Health Organisation
CoV	Coronaviruses
Mpro	main protease
RBD	receptor-binding domain
FP	fusion peptide
HR1	heptad repeat
TNF- α	tumour necrosis factor-α
IL	interleukin
MAPK	mitogen activated protein kinase
cox-2	cyclooxygenase-2
iNOS	inducible nitric oxide synthase
ROS	reactive oxygen species
ACE2	Angiotensin-converting Enzyme-2
ADMET	Absorption, Distribution, Metabolism, Excretion and Toxicity
ML	machine learning
clogP	Octanol-water partition coefficient
MWT	Molecular weight
RB	Number of rotatable bonds
AP	Aromatic proportion
MD	Molecular Dynamics
RMSD	Root Mean Square Deviation
RMSF	Root Mean Square Fluctuation
ROG	Radius of Gyration

---

no specific drug available for treatment. Integrating the traditional medicine systems in clinical practice will allow better healthcare outreach in urban, rural and remote areas alike.[1] In India, Siddha medicine, an ancient system of codified traditional medicine, that uses specific polyherbal formulations to treat several diseases including infections, was one of the preventive/therapeutic approaches during COVID-19 pandemic.[2,3] Siddha medicine, mainly associated with southern India, has its origins traditionally attributed to eighteen sages (*Siddhars*), the earliest of whom are believed to have lived several thousand years ago (in remote antiquity).[2] This system of medicine is also practiced in several south-east Asian countries – Sri Lanka, Malaysia, Singapore and Mauritius.[4]

The novel Coronavirus disease-2019 (COVID-19), caused by Severe Acute Respiratory Syndrome Coronavirus 2 (SARS-CoV-2), was declared a 'pandemic' by the World Health Organisation (WHO). Absence of targeted therapy took a huge toll of human lives pointing to an imminent need for finding safe and effective anti-viral agents. The use of herbal remedies as an adjuvant with drug treatment has additional positive effects and is likely to reduce COVID-19 severity in a relatively shorter time span.[5] Phytochemicals derived from medicinal plants and herbs are valuable alternatives for adjunct treatment of viral infections including COVID-19.[6,7]

Coronaviruses (CoV) are positive-sense single-stranded RNA viruses with specialized encasing proteins called Spikes (S), and the main protease (Mpro) involved in the processing of polyproteins translated from viral mRNA.[8,9] Spike, a class I viral fusion protein, folds into a trimer, and is made of two major components, namely S1 at the amino-terminus and S2 in the carboxy-terminus. S2 promotes membrane fusion, whereas S1 contains the receptor-binding domain (RBD). The spike protein exhibits two distinct forms during the viral entry process: (i) pre-fusion, which is the form observed on mature virions, and (ii) post-fusion, which is formed after membrane fusion.[10,11] After the virion has been attached to the host cell receptor (ACE-2), lysosomal proteases perform a second crucial cleavage at the S2′ cleavage site, allowing the internal fusion peptide (FP) to be released, the Spike protein envelope to fuse with the host membrane, and the transformation of S2 into the post-fusion structure.[12,13]

Despite the limited time of fusion intermediate phase, it is reported to be still long enough for its inhibitory peptides to bind with the pre-hairpin intermediate, and prevent formation of the six-helix bundle. Furthermore, it has been established that the heptad repeat (HR1) regions of several human CoVs as well as other viruses such as murine hepatitis virus are highly conserved, making them an attractive target for developing vaccines and drugs for pan-CoVs, including SARS-CoV-2.[14,15] The past and present occurrence of CoV infections, with potential for recurrence of its variants in future, has prompted serious investigation of conserved Spike protein (such as post-fusion S protein) as therapeutic target.[16,17]

Drug repurposing/repositioning have been employed for quickly identifying new uses of approved drugs to treat COVID-19 infected patients.[18,19] Natural products are also being evaluated for preventive management and immunity-boosting.[20] Phytochemicals target multiple pro-inflammatory and oxidative mediators such as tumour necrosis factor-α (TNF- α), interleukin (IL) β, IL-6, matrix, metalloproteinase (MMPs), nuclear factor kappa B, mitogen activated protein kinase (MAPK), cyclooxygenase-2 (cox-2), inducible nitric oxide synthase (iNOS) and reactive oxygen species (ROS), suggesting their benefit in mitigating coronavirus infection and its inflammatory consequences.[21,22]

In India, the Ministry of AYUSH (Ayurveda, Yoga and Naturopathy, Unani, Siddha and Homeopathy), Government of India, issued guidelines for the practice of the ancient systems of medicine as part of the COVID-19 holistic disease control and management.[23] Accordingly, the use of Kabasura Kudineer, a polyherbal Siddha medicine decoction, and few other Siddha formulations were recommended by public health authorities in southern India, on the basis of their effectiveness in boosting immunity and protection against respiratory diseases. A hospital based clinical trial reported favourable outcomes in asymptomatic and mild COVID-19 patients treated with fixed regimen of Siddha medicines which also included Kabasura Kudineer.[24] The polyherbal extract, Kabasura Kudineer showed anti-inflammatory effects in an *in vitro* cell culture model, suggesting its favourable modulation of inflammation associated with COVID-19 infection.[25] In the present study, the key bioactive constituents reported in Kabasura Kudineer formulation[2] were subjected to molecular docking against viral targets – Mpro and post-fusion spike protein, followed by molecular dynamics analysis and pharmacokinetic profiling.

2. Materials and methods

Combination of computational tools that include molecular docking, molecular dynamics simulations and MM-PBSA/MM-GBSA based free energy/entropy analysis yield several significant insights on ligand-protein binding interactions, binding stability and energy.[26–28] Here in our study, molecular docking of two major proteins involved in SARS-CoV-2 - host infection — (i) Main protease (PDB ID: 5RG1) and (ii) Spike protein (post-fusion hairpin confirmation (PDB ID: 1WYY)) was performed using Glide module of Schrodinger software. The selected 32 phytochemicals from Kabasura Kudineer formulations served as the candidate ligands for molecular docking with the viral protein targets as well as molecular dynamics studies. This was followed by druglikeness and solubility prediction of 32 test

ligands using machine learning algorithm (linear regression model). This was further validated using an online tool with additional pharmacokinetic profiling. Supplementary Fig. 1 presents the overall workflow of this study.

2.1. Selection of protein

Post-fusion Spike protein (PDB ID: 1WYY),[15] and Mpro (PDB ID: 5RG1)[29] of SARS-CoV were acquired from the protein data bank (www.rcsb.org). The PDB format of target proteins were downloaded and used for further studies.

2.2. Ligand preparation

A total of 32 ligands were chosen for molecular docking experiments in order to identify potent antiviral agents, particularly for COVID-19. Kabasura Kudineer Chooranam is a polyherbal formulation made up of fifteen different herbal ingredients that are blended in equal amounts and then decocted.[30] The specified 3D chemical structures of the selected compounds were imported using the PubChem (Supplementary Table 1). The bioactives include β-Sesquiphellandrene, β-Bisabolene, Geranial, Piperine, Piperlonguminine, Eugenol, β-Caryophyllene, Stigmasterol, Squalene, γ-Sitosterol, Andrograpanin, 5-Hydroxy-7-8-Dimethoxyflavone, Lupeol, Betulin, Gallic acid, Carvacrol, Cirsimaritin, Chrysoeriol, 6-Methoxygenkwanin, Luteolin, Costunolide, Elemol, Tinosponone, Bharangin, Scutellarein, Magnoflorine, Cycleanine, Cyperene, β-Selinene, Quercetin, Andrographolide, Ursolic acid.[2,18,31] During the ligand preparation process, all potential conformations were considered. The ligands were then subjected to further pre-docking preparations including addition of hydrogens, followed by minimization and optimization using Optimized Potentials for Liquid Simulations (OPLS3e) force field of Schrodinger software.
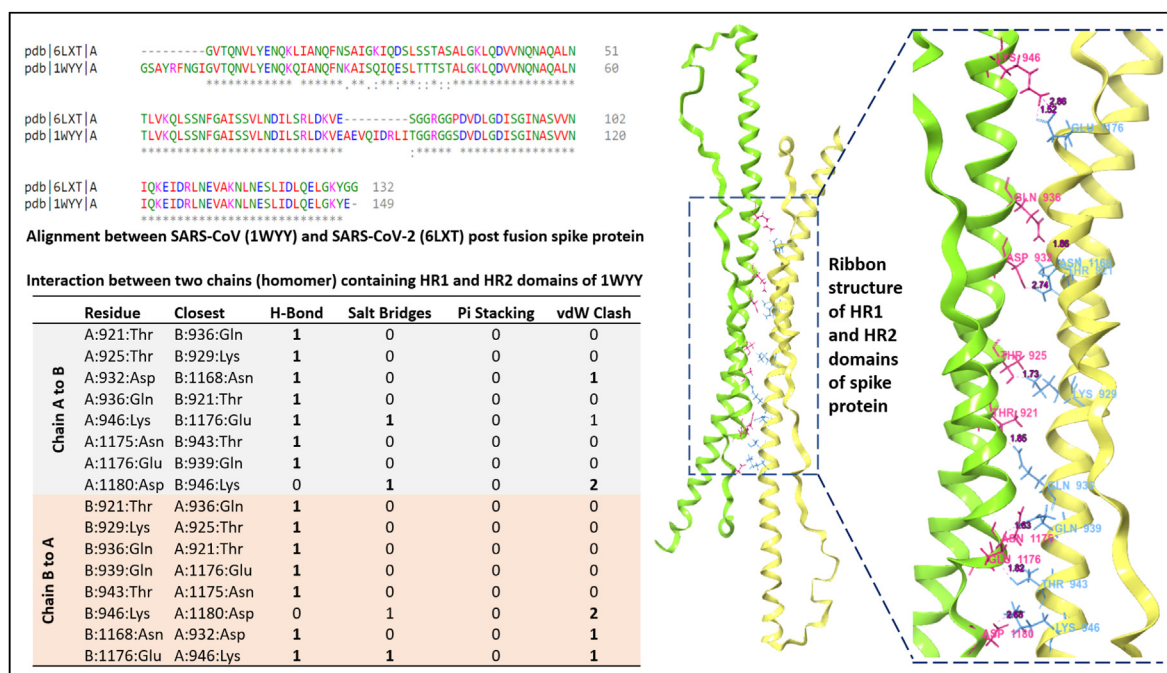
2.3. Protein preparation

To evaluate the antiviral activity of phytoconstituents in the Siddha formulation Kabasura Kudineer Chooranam, we selected Spike glycoprotein (post fusion hairpin confirmation), a vital target for developing therapeutics, vaccines, and diagnostics in SARS-CoV-2 management.[15] The single receptor-binding domain (RBD) of the Spike glycoprotein of SARS-CoV-2 interacts with the ACE2 (Angiotensin-converting Enzyme-2) receptor on the host cell with high affinity, making it an attractive anti-viral target. The 3D structures of the post-fusion Spike glycoprotein (PDB ID: 1WYY) and main protease (PDB ID: 5RG1) were selected, and obtained from Protein Data Bank. The X, Y and Z coordinates of 5RG1 used for glide docking are X = 9.53, Y = 0.93, Z = 22.57. The protein was prepared by adding the polar hydrogens and by removing the water molecules, followed by minimization and optimization using Schrodinger protein preparation wizard. In order to score the ligand poses with gradually higher accuracy, many different sets of fields were employed to represent the shape and features of the receptor on a grid.

2.4. Molecular docking studies

Molecular docking is a structure-based design method that uses low energy conformation to find critical amino acid interactions between a protein and a ligand.[32] The molecular docking was performed using Glide module of Schrodinger software. For the 32 phytochemical ingredients in the Siddha formulation Kabasura Kudineer Chooranam, molecular docking was performed. The phytochemical analogues were docked with Spike glycoprotein (post-fusion) (PDB: 1WYY), and the main protease (PDB: 5RG1) using the Glide module of Schrodinger.[33] The Spike glycoprotein of the SARS-CoV-2 virus attaches to human cells, making it a vital target for developing potential therapeutics. In this post-fusion core of S2 subunit, the HR1 and HR2 domains interact to form a coiled complex strong enough to support viral fusion. As the SARS spike has been studied extensively during its outbreak and the experimental structure was well established, the entire analysis in this study was carried out in the SARS spike. However, to understand the similarity of post-fusion spike protein in both viruses, our analysis from aligning both proteins using Clustal omega (https://

Alignment between SARS-CoV (1WYY) and SARS-CoV-2 (6LXT) post fusion spike protein

Interaction between two chains (homomer) containing HR1 and HR2 domains of 1WYY

	Residue	Closest	H-Bond	Salt Bridges	Pi Stacking	vdW Clash
Chain A to B	A:921:Thr	B:936:Gln	1	0	0	0
	A:925:Thr	B:929:Lys	1	0	0	0
	A:932:Asp	B:1168:Asn	1	0	0	1
	A:936:Gln	B:921:Thr	1	0	0	0
	A:946:Lys	B:1176:Glu	1	1	0	1
	A:1175:Asn	B:943:Thr	1	0	0	0
	A:1176:Glu	B:939:Gln	1	0	0	0
	A:1180:Asp	B:946:Lys	0	1	0	2
Chain B to A	B:921:Thr	A:936:Gln	1	0	0	0
	B:929:Lys	A:925:Thr	1	0	0	0
	B:936:Gln	A:921:Thr	1	0	0	0
	B:939:Gln	A:1176:Glu	1	0	0	0
	B:943:Thr	A:1175:Asn	1	0	0	0
	B:946:Lys	A:1180:Asp	0	1	0	2
	B:1168:Asn	A:932:Asp	1	0	0	1
	B:1176:Glu	A:946:Lys	1	1	0	1

Fig. 1. Structural characterization of post-fusion spike protein of SARS (1WYY) and SARS-CoV-2 (6LXT), its alignment and interaction between the chains. The two chains of 1WYY protein have been depicted in green (Chain A) and yellow (Chain B).

www.ebi.ac.uk/Tools/msa/clustalo/) shows highly conserved sequences (Fig. 1). Upon observing the interactions between the domains, a total of eight residues of each chain interact with each together (Fig. 1). This analysis provides insight into the active site to target while carrying out the molecular docking studies.

A grid was generated using the co-ordinates of native ligand for Main protease. Since spike glycoprotein (PDB: 1WYY) does not possess any co-crystal ligand, we performed site map analysis to predict the active sites.[34] Interestingly, the highly scored active site region (site-1) (Supplementary Table 2), has interacting residues between HR1 and HR2 domains (Fig. 1). The residues include Ser924, Gly928, Asp932, Gln1161, Asn1168 and Ile1164. Therefore, the site-1 was chosen in order to generate a grid-box for docking studies.

2.5. Molecular dynamics studies

Molecular dynamics studies were performed using the Desmond module of Schrödinger software (Academic, version 2020.4).[35] Initially, the protein-ligand complex (PLC) was solvated using water molecules via the system builder wizard of the Schrödinger software. The solvent system used for the study was transferable intermolecular potential 3P (TIP3P).[36] The simulations were performed in an orthorhombic box with the dimensions of $10 \times 10 \times 10$ Å, and periodic boundary conditions were used. In order to neutralize the excess charge on the system, a total of 13 Na^+ ions in the case of spike protein (PDB: 1WYY) and 2 Na^+ ions in the case of main protease (PDB: 5RG1) were added. The salt concentration was kept to be 0.15 M. The Optimized Potentials for Liquid Simulations 2005 (OPLS 2005), which is the enhanced version of the OPLS/AA (All-Atom) force field as implemented in Schrödinger,[37] was used for all the molecules. The complete model system was minimized for 100 ps, and its trajectory was used for performing molecular dynamics study. The dynamics studies were carried out for 100 ns, and the recording interval was set to 100 ps such that the total number of frames for complete studies are 1000. Constant-temperature, constant-pressure ensemble (NPT ensemble) was chosen at 310.15 K temperature and 1.013 bar pressure. The temperature was controlled using Nosé−Hoover chain thermostat and pressure was controlled using Martyna-Tobias-Klein barostat with a time constant of 1 ps and 2 ps, respectively. The time step used in the simulations was 2 fs.[38]

2.6. MM-PBSA analysis

The Molecular Mechanic/Poisson-Boltzmann Surface Area (MM-PBSA) calculations were performed using gmx_MMPBSA package.[39,40] The molecular dynamics trajectories were first converted from Schrodinger to GROMACS format using Intermol software.[41] The MM-PBSA method was employed to calculate the binding free energy of the protein-ligand complex. The calculation employed the Poisson-Boltzmann method with dielectric model (ipb = 2) and the non-polar solvation model (inp = 1). The ionic strength of the medium was maintained at 0.15 M at a temperature of 310 K. Entropy, expressed in terms of $-T\Delta S$ was calculated using interaction entropy (IE) method. The calculations were performed on last 30 ns of the molecular dynamics trajectories to calculate the change in binding free energy of both the target protein-ligand complexes. We divided the data into several batches to calculate the better averaging of entropies as discussed previously.[42]

2.7. Evaluation of drug likeness and toxicity of ligands

The commonly followed Lipinski's rule or Rule-of-Five is used for evaluating the drug likeness of compounds. Such drug likeness prediction is mainly based on the Absorption, Distribution, Metabolism, Excretion and Toxicity (ADMET) that is also known as the pharmacokinetic profile. Here we have used machine learning (ML) based approach and an online tool pkCSM[43] for pharmacokinetic profiling. According to Lipinski's rule, the molecular weight of the compounds should be less than <500 Da, octanol-water partition coefficient (LogP) < 5, hydrogen bond donor ≤5, hydrogen bond acceptor should be ≤ 10. According to Lipinski's rule the compound should not have more than one violation.

2.8. Predicting the solubility of molecules

We applied Linear Regression to predict the solubility of molecules as it is an important physicochemical property in drug discovery, design and development (Supplementary Fig. 2 (a)). To predict LogS (log of the aqueous solubility), the study by Delaney[44] makes use of 4 molecular descriptors:

1) clogP (Octanol-water partition coefficient)
2) MWT (Molecular weight)
3) RB (Number of rotatable bonds)
4) AP (Aromatic proportion = number of aromatic atoms/total number of heavy atoms)

The work of Delaney provided the following linear regression equation to predict aqueous solubility directly from molecular structure[44]:

$$Log(S) = 0.16 − 0.63 \text{ clogP} - 0.0062 \text{ MWT} + 0.066 \text{ RB} - 0.74 \text{ AP}$$

LogS is the maximum dissolved concentration in a solvent at any given conditions. It determines intestinal absorption and oral bioavailability i.e., lower the solubility resulted into lower oral bioavailability. In other words, higher the solubility lesser will be its permeability. The compound should have good solubility for intravenous formulation.

We determined the ADME properties using Lipinski's Rule of 5 and built a regression model using Machine Learning with Python,[45] and the workflow is depicted in Supplementary Fig. 2 (b).

3. Results and discussion

Siddha system of medicine is one of the oldest documented systems in the world and has been utilized successfully by human civilization for ages to treat a variety of ailments, for instance the use of Kabasura Kudineer during influenza outbreaks.[46] Moreover, during the Dengue fever outbreaks in India, Nilavembu Kudineer, a Siddha herbal preparation has been employed to prevent and control the potential morbidity caused by this viral fever. In a recent *in vitro* study, the water extract of Kabasura Kudineer was able to diminish viral RNA of SARS-CoV-2 [47]. Siddha herbal formulations have demonstrated their medicinal efficacy against a wide range of infectious diseases such as tuberculosis and viral diseases such as influenza, dengue, chikungunya, mumps and others.[46−49] The known pharmacological effects of the major phytoconstituents in Kabasura Kudineer have been listed in Supplementary Table 3. Here, we present the exact binding pattern of the bioactives in Kabasura Kudineer against the key molecular targets in SARS-COV-2, using computational approaches.

3.1. Docking validation

Once the proteins were prepared using protein preparation wizard, the co-crystal ligands were extracted from the complex and redocked in the same active site. This resulted in the Root Mean
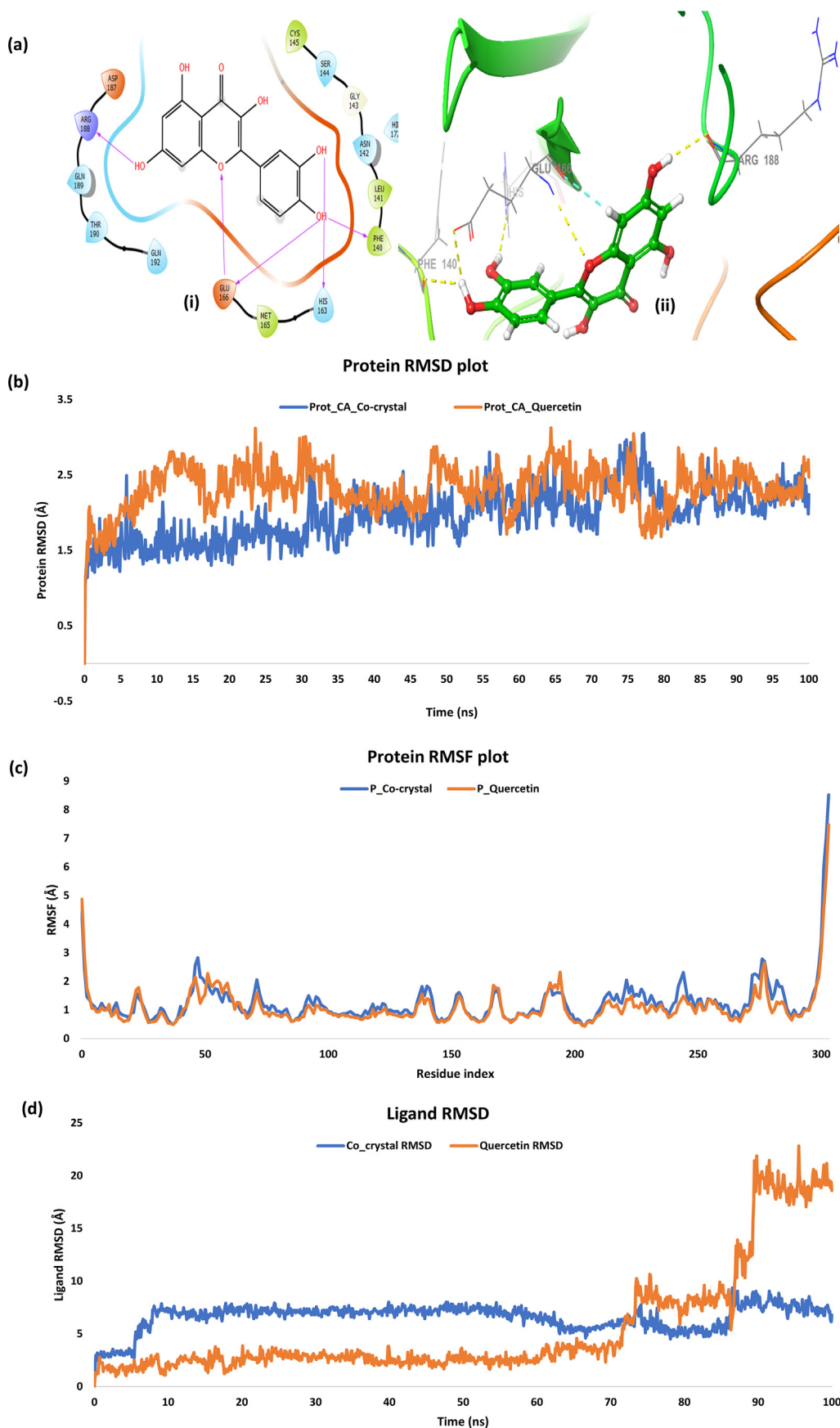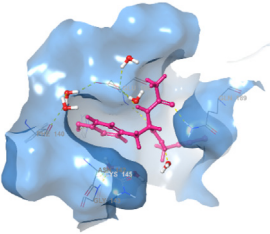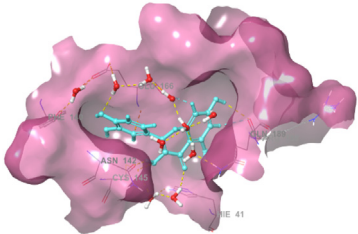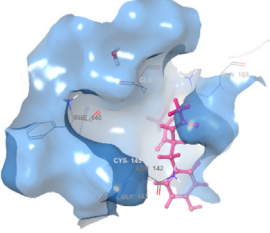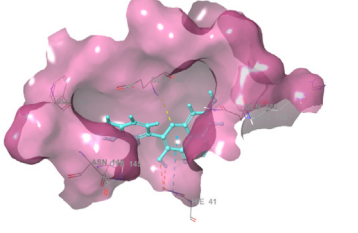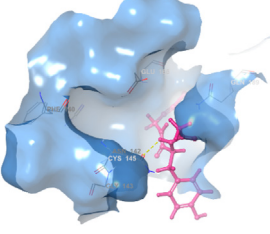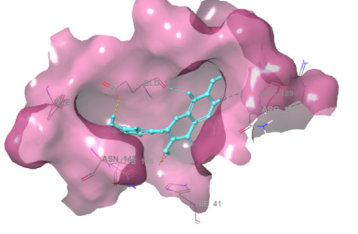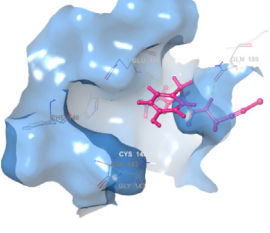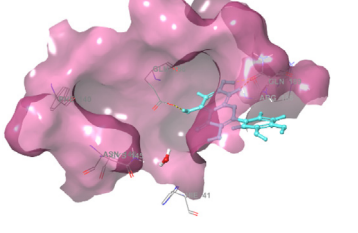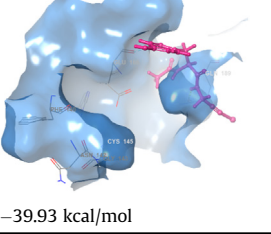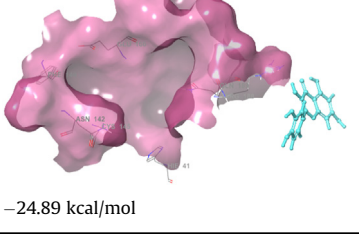
Fig. 2. **(a)** Docking image of Quercetin against Main protease (i) 2D representation (ii) 3D representation **(b)** RMSD plot representing the deviation in 5RG1 during the simulation time **(c)** RMSF plot representing the fluctuations of 5RG1 residues during simulation **(d)** RMSD plot representing the deviation of co-crystal ligand and quercetin during the simulation time.

Square Deviation (RMSD) of 0.98 Å which validates our docking protocol. The RMSD of co-crystal ligand of Main protease is shown in Supplementary Fig. 3. In order to validate the top scoring ligand's binding with post fusion spike protein which lacks a co-crystal ligand in its crystal structure, we chose a comparable spike post-fusion spike protein (6LXT) crystal structure that has been recently reported with respect to SARS-CoV-2 in the year 2020.[17] Importantly, we superimposed the two crystal structures (1WYY and 6LXT) and found strong interactions between the domains, wherein eight residues from HR1 interact with ten residues from the HR2 domain. Among these, most interactions are H-bonded (Fig. 1). This analysis confirmed the active binding site of our ligands to the protein target when carrying out docking studies, based on published report.[17]

Table 1
Time based free-energy calculations and conformations of quercetin in the case of main protease along with the co-crystal ligand.

Time interval	MM-GBSA ΔG bind	
	5RG1	
	Co-crystal	Quercetin
Docked pose	−57.47 kcal/mol	−47.81 kcal/mol
25ns	−65.59 kcal/mol	−46.06 kcal/mol
50ns	−32.83 kcal/mol	−37.83 kcal/mol
75ns	−60.24 kcal/mol	−25.93 kcal/mol
100ns	−39.93 kcal/mol	−24.89 kcal/mol

3.2. Docking and MD analysis

3.2.1. Analysis with respect to main protease (PDB: 5RG1)

From the docking results obtained against 5RG1, a total of 14 natural ligands showed better glide score than co-crystal ligand. Among these, Quercetin is the highest with Gscore of −7.772 kcal/mol while that for co-crystal ligand was −5.281 kcal/mol. Quercetin formed a total of six H-bond interactions each with Phe140, His163, Arg188 and two interactions with Glu166 (Fig. 2a and b). The two residues His163 and Glu166 were also seen with the co-crystal ligand within the active site (Fig. 2 (a)). Hence, the greater number of H-bond interactions observed with Quercetin resulted in better binding than the co-crystal ligand.

The MD results indicated that the protein has minor fluctuations as the RMSD was less (<3.5 Å). The protein residue showed less deviation in presence of both the ligands, this indicates the stability of protein for complete 100 ns (Fig. 2 (b)). Further, Root Mean Square Fluctuation (RMSF) plot did not show major deviations of the active site residues (Fig. 2 (c)). In case of ligand RMSD plot, the co-crystal ligand slightly fluctuated until 4 ns and from 5 ns, the confirmation changed resulting in higher RMSD to 5 Å, beyond it the ligand remained stable until 87 ns with few fluctuations. However, during the end of the simulation, the RMSD varied between 10 Å and 6 Å. Change in free energy and the conformations of the ligand at intervals of 25 ns each are shown in Table 1. Similar trend was observed with Quercetin but had lower RMSD, ranging between 1 and 4 Å, lower than co-crystal ligand. Beyond 70 ns, the ligand started moving out of the active site increasing the RMSD gradually and decreasing the free energy of the complex system; and later it completely moved out of the active site pocket (Fig. 2 (d)) as shown in Table 1 of time-based conformations. The residues that predominantly interacted in the docking study were His41, Phe140, Ser144, His163, Glu166, Asp187, Asp188 and these residues retained during the MD studies (Fig. 3 (a and b)). Among

these residues, Asp187, Glu166 and Ser144 contributed for 36%, 33% and 30% of interactions respectively, during the entire simulation time. While other residues such as His163, Gln192, Arg188 contributions were less than 20% (Fig. 3).

3.2.2. Analysis with respect to post fusion spike protein (PDB: 1WYY)

Docking studies were performed against post-fusion Spike protein of SARS-CoV-2 (PDB: 1WYY). The results revealed that Gallic acid exhibited least binding energy with glide score of −6.721 kcal/mol. It formed a total of five H-bonds with the residues of both the chains (Fig. 4 (a)). The interactions were formed due to hydroxy groups present on the ligand. In addition, both the chains participated in interacting with the residues. The docking results of 32 ligands along with co-crystal ligand against main protease as well as post fusion Spike protein are presented in Table 2 and Fig. 5.

The complete summary of the protein residues that participated in interactions with 5RG1 and 1WYY are tabulated in Table 3.

In the beginning of the MD studies, huge variations were seen between protein and the ligand (Gallic acid). The protein residue had greater fluctuations up to 10 ns resulting in higher RMSD of 10 Å and later attained equilibrium with minor fluctuations variating between 10.5 Å and 13 Å (Fig. 4 (b)). The reason for high RMSD is due to the residues between 24 and 90, 120–135 and 180–220 had huge fluctuations (Fig. 4 (c)). In addition, ligand shows high RMSD at the beginning of 10 ns during which it tends to change its conformations continuously and moved out of the active site pocket (Fig. 4 (b)). The free energy of the docked pose was −32.04 kcal/mol, ranged with ±5.0 kcal/mol during the simulation and the last frame of the study (frame 1001) was −20.54 kcal/mol. This indicates the ligand's stability as it did not leave the active site pocket for the complete simulation (Table 4). Despite moving out, the ligand had strong contacts with
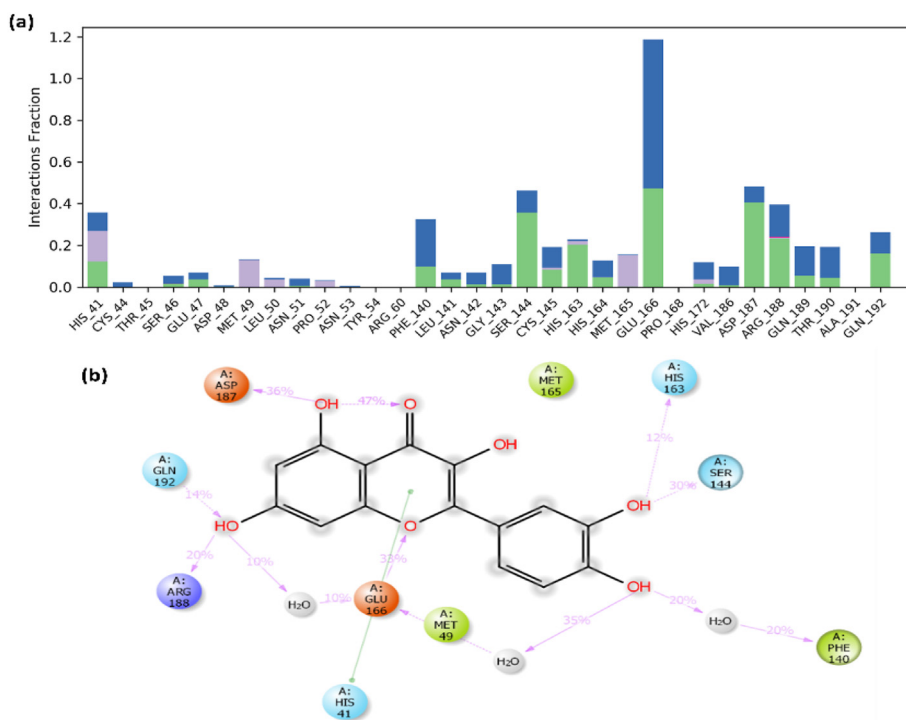
Fig. 3. (a) Protein-ligand contact plot representing the 5RG1 residues involved during interactions with Quercetin **(b)** Protein-ligand contacts representing the percentage contribution of residual interactions with Quercetin.
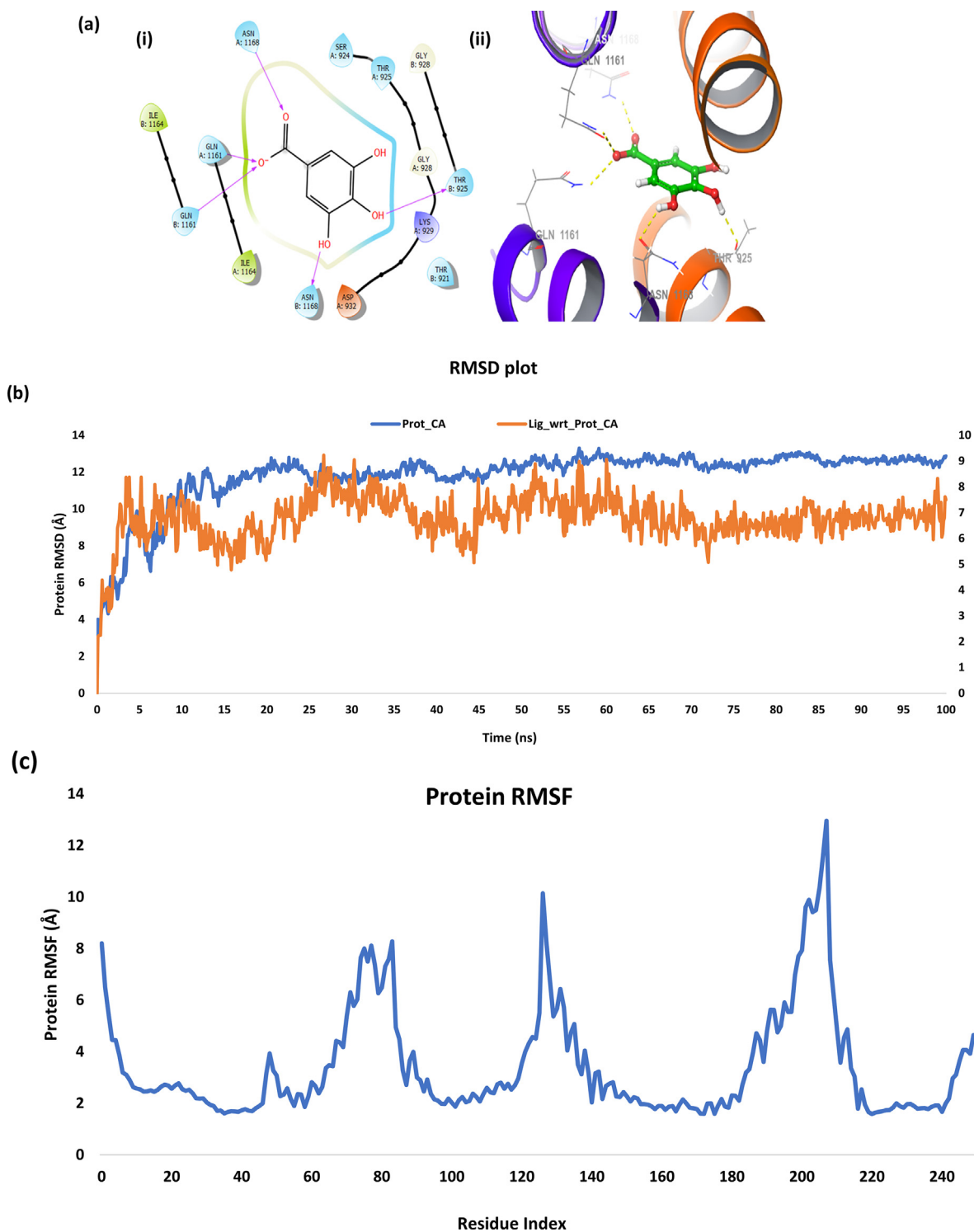
Fig. 4. (a) Docking image of gallic acid against post fusion spike protein (i) 2D representation (ii) 3D representation **(b)** RMSD plot representing the deviation in post-fusion Spike protein (1WYY) and Gallic acid during the simulation time **(c)** RMSF plot representing the fluctuations of post-fusion Spike protein (1WYY) residues during simulation.

Asp932, Lys929 and Thr925 during most of the simulation time. The other residues such as Thr921, Ser924, Gly928, Gln931 and Gln1161 had interaction with gallic acid for 50% of the simulation (Fig. 4 (a)). Asp932 alone contributed for 99% interaction with the active site residues, while the other residues mostly formed water mediated interactions (Fig. 4 (a)).

In order to address the thermodynamic stability of the protein-ligand complex and to validate our docking results, we calculated the binding free energy of the protein, ligand and protein-ligand complex using MM-PBSA method. The resulting change in binding free energy of the protein-ligand complex was then calculated using the following equation:

$$\Delta G_{binding} = G_{complex} - \left(G_{protein} + G_{ligand} \right)$$

Fig. 5. (a) Protein-ligand contact plot representing the 1WYY residues involved during interactions with Gallic acid **(b)** Protein-ligand contacts representing the percentage contribution of residue - interactions with Gallic acid.

In the given equation, $G_{complex}$ represents the energy of the protein-ligand complex formed by the lead phytochemical and the test protein. $G_{protein}$ and G_{ligand} represent the energy of the protein and the ligand, respectively, in a water-surrounded environment.

The contribution of various energies to the change in binding free energies is given by the following equation:

$$\Delta Gbind = (\Delta Eel) + (\Delta Evdw) + (\Delta Gsol) + (\Delta GSASA) - (T\Delta SIE)$$

The contributions of various terms to the binding free energies are shown in Table 5, where each value represents an average of three time points of the simulations. The binding free energy of both the complex shows a negative value indicating the favourable interaction between the protein-ligand complex.

3.3. ML based prediction of drug likeness

Lipinski's Rule of 5 is an important consideration for determining whether a chemical entity would be an orally active drug suitable for human consumption, based on evaluating its physicochemical properties. This rule evaluates several parameters or descriptors that are relevant to drug design. Lipinski's rule states that compounds must have molecular mass of <500 Da, not >5 H-bond donors, not >10 H-bond acceptors, and an O/W partition coefficient (log P) < 5, wherein if a molecule or compound violates more than three descriptor parameters, then it does not meet the requirements for drug likeness and is not considered for further drug development. Using ML based approach, the drug likeness properties of the 32 phytoconstituents were assessed by Lipinski rule of five, Veber Ghose, Muegge, and Egan rules based on several physicochemical properties such as molecular weight, proportion of aromatic groups and solubility (Supplementary Table 6, Fig. 6). The present analysis revealed that out of 32 phytochemicals present in Kabasura Kudineer, 31 molecules showed no violations of this rule indicating favourable pharmacological application, both in the polyherbal formulation as well as individual bioactive molecules. The molecule that showed exception to the rule was found to be Cycleanine.

The ML-based pharmacological suitability of the molecules was further confirmed and validated with other physiologically significant ADMET parameters using an online tool, pkCSM, which are discussed below.

Table 2

Molecular docking analysis of phytoconstituents in polyherbal Siddha formulation Kabasura Kudineer against Mpro (PDB ID: 5RG1) and post-fusion Spike Protein (PDB ID: 1WYY).

Compound name	5RG1		1WYY	
	Glide Gscore	Glide energy	Glide Gscore	Glide energy
5-Hydroxy-7,8-Dimethoxyflavone	−7.042	−37.185	−2.072	−24.08
6-Methoxygenkwanin	−6.448	−46.265	0	0
Andrograpanin	−5.664	−30.553	0	
Andrographolide	−5.871	−27.108	0	0
Beta sitosterol	−4.046	−27.849	0	0
Beta-Bisabolene	−4.749	−22.249	−2.625	−22.348
Beta-Selinene	−4.802	−29.107	−4.067	−12.871
Beta-Sesquiphellandrene	−4.487	−23.381	−3.292	−25.224
Betulin	−4.293	−30.409	−1.896	−24.703
Bharangin	−4.808	−31.5	0	0
Carvacrol	−4.9	−22.969	−1.157	−22.427
Chrysoeriol	−7.119	−44.112	−4.804	−29.702
Chrysoeriol	−6.344	−34.829	−2.484	−13.093
Cirsimaritin	−6.264	−45.264	0	0
Costunolide	−4.527	−31.372	−3.661	−13.402
Cycleanine	−3.018	−37.133	0	0
Cyperene	−3.857	−24.535	0	0
Elemol	−5.293	−27.148	−4.23	−24.016
Eugenol	−4.938	−28.121	−3.423	−31.716
Gallic Acid	−6.443	−25.711	−6.721	−30.242
Geranial	−3.296	−21.775	−3.861	−22.873
Lupeol	−3.77	−34.863	0	0
Luteolin	−7.297	−43.095	−3.446	−12.114
Magnoflorine	−6.049	−37.133	0	0
Piperine	−5.509	−36.169	−4.143	−36.172
Piperlonguminine	−4.636	−31.036	−5.271	−36.857
Quercetin	−7.922	−44.697	−4.041	−29.489
Scutellarein	−6.902	−43.145	−2.4	−11.454
Squalene	−5.389	−41.588	2.124	−27.187
Stigmasterol	−3.999	−31.394	0	0
Tinosponone	−6.084	−41.358	0	0
Ursolic Acid	−3.633	−35.801	0	0
Co-crystal	−5.281	−42.434	–	–

Table 3

Docking results summary of the top scoring ligands Quercetin and Gallic acid.

S. no	Target	Chain	Ligand	Residues	Interaction type	Bond length (Å)
1.	5RG1	A	Quercetin	Phe140; His63; Glu166; Arg188	H-bond	2.53; 2.27; 2.12, 2.76; 2.10
2.	1WYY	A	Gallic acid	Gln1161; Asn1168	H-bond	2.29, 2.20
		B		Thr925; Gln1161; Asn1168	H-bond	1.77; 2.29; 2.07

3.4. In silico predicted pharmacokinetic (ADMET) profiling of the phytoconstituents

Using the online pkCSM webserver, pharmacokinetic properties of phytochemical ingredients in Siddha polyherbal formulation Kabasura Kudineer Chooranam were assessed. Lupeol, Betulin, Ursolic acid, Geranial, Costunolide, Tinosponone, Hydroxy-7-8-Dimethoxyflavone, Andrograpanin, beta-Selinene, beta-Caryophyllene, beta-Sesquiphellandrene, and Stigmasterol had the maximum gastrointestinal absorption, tissue distribution (Vd), and good total clearance, according to the pharmacokinetic properties analysis (Table 6). The bioavailability of Lupeol, Ursolic acid and Betulin components in the Kabasura Kudineer formulation is 100%, while the oral bioavailability of the remaining compounds is >80%.
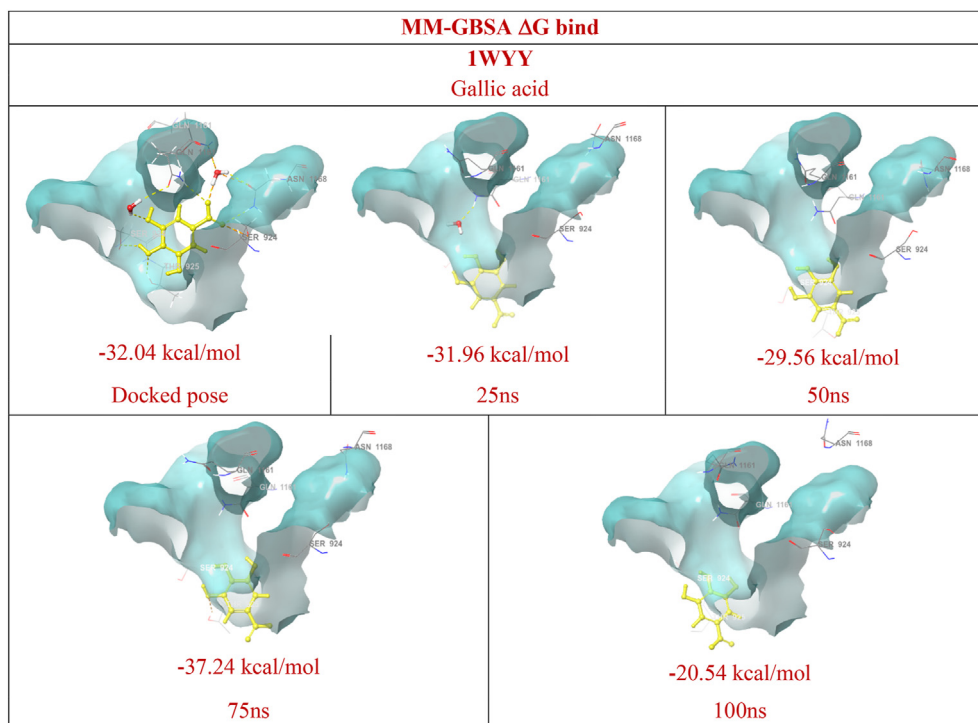
The 32 phytoconstituents of the Siddha polyherbal formulation (Kabasura Kudineer) were analysed for Cytochrome-P450 and P-glycoprotein substrate/inhibitor roles, by pkCSM based simulation studies (Table 6). The findings revealed that most of the phytoconstituents have low CYP inducing and P-gp compatibility properties. Bharangin, Andrograpanin, Cycleanine, Betulin, Lupeol, Stigmasterol, and gamma-Sitosterol may be metabolised by the CYP3A4 enzyme. Furthermore, there was no drug-drug interaction with Luteolin, Scutellarein, Chrysoeriol, Cirsimaritin, 6-Methoxygenkwanin, 5-Hydroxy-7-8-Dimethoxyflavone, Cyperene, beta-Selinene, and Magnoflorine due to inhibition of Cytochrome-P450 (CYP). Importantly, Gallic acid, Quercetin, Andrographolide, Chrysoeriol, Cirsimaritin, 6-Methoxygenkwanin, 5-Hydroxy-7-8-Dimethoxyflavone, Bharangin, Cyperene, Andrograpanin, Squalene, Lupeol, Stigmasterol, gamma-Sitosterol show no toxicity.

In the recent viral pandemic scenario, several systems of traditional medicine offered treatment benefits to tackle the infection, boost immunity and prevent clinical complications. The in silico approach of mechanistically validating the traditionally used phytochemical polyherbal formulations is an efficient way to curtail the disease transmission, as evidenced by published reports on traditional Chinese formulations, and Indian medicinal formulations from Ayurveda and Siddha systems, including Kabasura Kudineer decoction.[50–53] A wide array of computational tools are currently available for accurate predictions, which were employed in this study, to better understand the anti-viral efficacy of Kabasura Kudineer.

In the present study, molecular docking and molecular

Table 4
Time-dependent free energy and conformations of gallic acid in the case of post-fusion spike protein.

| MM-GBSA ΔG bind |
| 1WYY |
| Gallic acid |

-32.04 kcal/mol — Docked pose

-31.96 kcal/mol — 25ns

-29.56 kcal/mol — 50ns

-37.24 kcal/mol — 75ns

-20.54 kcal/mol — 100ns

dynamics simulation analysis revealed the significant binding efficacy of both quercetin and gallic acid against the selected viral targets such as Mpro and pan-coronavirus post fusion Spike protein, respectively. This partly explains the mechanistic basis for the antiviral efficacy of the traditional polyherbal formulation. Previously research groups have suggested favourable modulation of SARS-CoV-2 spike protein and destabilization of its interaction with ACE2 receptor.[54] A recent review highlighted the broad spectrum anti-viral efficacy of quercetin, wherein (a) quercetin is reported to be effective against several viruses, including coronavirus, and (b) its anti-coronavirus action is exerted by multiple mechanisms, including targeting of Mpro and viral-host interaction. It was suggested that Quercetin and its analogues showed potent antioxidant and broad-spectrum antiviral activity *in vitro* and could be used for prophylactic purpose as well as for treating viral infections by using it in combination with appropriate drugs. The latter combination therapy would also minimize the drug related side effects.[55,56] Our lab recently reported the anti-obesity efficacy of quercetin, which points to the ability of such natural products to deal with the infection amidst comorbidities.[57]

Gallic acid and its derivatives are reported to have diverse protective properties that include antioxidant, anti-inflammatory, and anti-viral properties (against several viruses including hepatic C virus, coronavirus).[56,58,59] Further, Gallic acid is also reported to have protective effects on pancreatic islets, renal and hepatic cells, thereby reducing the diabetes complications. The suggested mechanisms are by increasing the GLUT4 protein expression in skeletal muscles, lipid profile improvement and an increase in insulin production.[60] Thus, Gallic acid cannot only mitigate the viral infection but also protect against the well-known co-morbidities such as diabetes that otherwise can result in clinical complications. Considering that the post fusion Spike protein is reported to be

Table 5
Summary of MM-PBSA analysis for post-fusion spike protein (1WYY) and main protease (5RG1).

	1WYY	5RG1
$\Delta E_{VDWAALS}$ (kcal/mol)	−18.30 ± 2.09	−29.92 ± 2.38
ΔE_{EL} (kcal/mol)	54.34 ± 11.82	−19.82 ± 6.49
ΔE_{PB} (kcal/mol)	−53.74 ± 11.55	35.89 ± 6.33
ΔE_{SASA} (kcal/mol)	−1.96 ± 0.05	−2.82 ± 0.14
ΔG_{TOTAL} (kcal/mol)	−19.66 ± 3.36	−16.66 ± 4.00
$-T\Delta S$ (kcal/mol)	11.36 ± 2.06	6.90 ± 1.92
ΔG_{IE} (kcal/mol)	−7.13 ± 4.16	−6.82 ± 4.63

conserved across several viruses, our present findings point to the versatility of the identified top scoring lead molecules, including gallic acid against 1WYY.

A clinical trial that compared two Siddha formulations (Nilavembu Kudineer and Kabasura Kudineer) that have been used for controlling other viral infections such as dengue and chikungunya, yielded favourable anti-COVID results when administered alongside standard allopathic treatment.[61] In their study, while both the polyherbal decoctions reduced SARS-CoV-2 load, time of hospital stay, and other parameters, Kabasura Kudineer fared better statistically. Taken together, the phytoligands in Kabasura Kudineer present substantial evidence for anti-viral efficacy.

4. Conclusions

There is an imminent need for target based anti-viral drugs that are safe and effective. The outcomes here substantiate the mechanistic basis of a traditional polyherbal formulation for its efficacy against COVID-19 respiratory infection and its potential to be
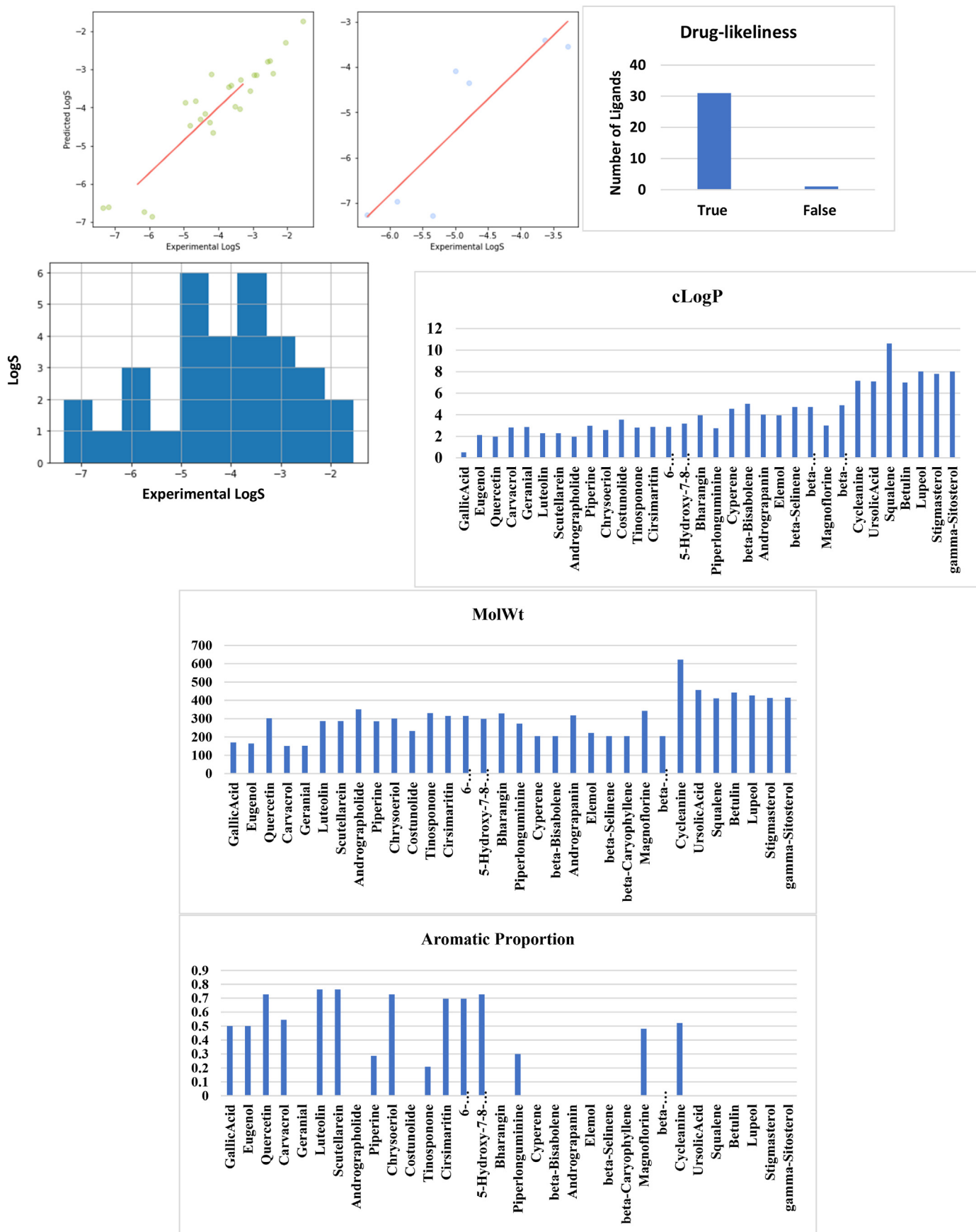
Fig. 6. ML-based comparative analysis of the 32 phytoconstituents of polyherbal formulation Kabasura Kudineer for their drug likeness based on clogP, MWT, Rotational bond, Aromatic proportion.

Table 6
In silico predicted pharmacokinetic parameters (ADMET) of the phytoconstituents from Kabasura Kudineer.

Para meters	Absorption						Distribution				Metabolism		Excretion		Toxicity			Lipinski's rule of five					
	Water solubility (log mol/L)	Caco2 permeability (log cm/s)	Intestinal absorption (%human)	Skin Perme ability (log Kp)	P-glyco protein substrate	P-glyco protein inhibitor	VDss (human) (log L/kg)	Fraction unbound (human) (Fu)	BBB perme ability (log BB)	CNS perme ability (log PS)	CYP sub strate	CYP inhibi tors	Total Clearance (log ml/min/kg)	Renal OCT2 substrate	AMES toxicity	Hepato toxicity	Skin Sensiti zation	Mole cular Weight	LogP	Rotatable Bonds	Acce ptors	Donors	Surface Area
Gallic acid	−1.91	−0.03	40.15	−2.74	N	N	−0.27	0.37	−1.42	−4.13	N	N	0.62	N	N	N	N	170.12	0.502	1	4	4	67.13
Quercetin	−3.00	0.29	74.9	−2.73	Y	N	0.11	0.09	−1.57	−3.41	N	N	0.55	N	N	N	N	302.24	1.99	1	7	5	122.11

Abbreviations: Caco2: Cancer coli-2, VDss: Volume of Distribution at Steady State, BBB: Blood-brain barrier, CNS: central nervous system, CYP: Cytochromes-P450, OCT2: Organic Cation Transporter. The *in-silico* ADMET prediction was performed using pkCSM web server.

considered for adjunct therapy. Such bioactives with pleiotropic beneficial effects help mitigate the acute condition and may also offer protection against co-morbidities and averting other clinical complications. The top-scoring bioactive molecules (Quercetin and Gallic acid with strong binding affinity for Mpro and post fusion Spike protein, respectively) in Kabasura Kudineer show promise as versatile lead-molecules for antiviral pharmacotherapy.

Authors contribution

SKM: Original draft, *in silico* analysis, molecular docking and ADMET analysis, illustrations.

MMR: Molecular dynamics studies, reviewing and editing.

AK: *In silico* molecular docking and ML-based ADMET analysis, manuscript preparation.

KR: Literature review, molecular docking and analysis.

MK: Conceptualization, data curation and analysis, reviewing and editing.

MG: *In silico* molecular simulations, MM-PBSA analysis and interpretation, reviewing and editing.

SM: MD data curation and analysis, reviewing and editing.

PRD: Conceptualization, data curation and analysis, reviewing and editing.

Declaration of competing interest

The authors declare no conflict of interest.

Acknowledgements

Appendix A. Supplementary data

Supplementary data to this article can be found online at https://doi.org/10.1016/j.jtcme.2023.07.004.

References

1. Sen S, Chakraborty R. Revival, modernization and integration of Indian traditional herbal medicine in clinical practice: importance, challenges and future. *J Tradit Complement Med*. 2017;7(2):234—244. https://doi.org/10.1016/j.jtcme.2016.05.006.
2. SIDDHA SYSTEM OF MEDICINE SIDDHA SYSTEM OF MEDICINE SIDDHA SYSTEM OF MEDICINE SIDDHA SYSTEM OF MEDICINE SIDDHA SYSTEM OF MEDICINE The Science of Holistic Health. Published online www.ayush.gov; 2019. Accessed November 13, 2022.
3. Zysk KG. Some reflections on siddha medicine in tamilnadu. *Indian J Hist Sci*. 2009;44(2):199—208, 10.1016%2Fj.jtcme.2022.01.002.
4. Jabaris SSL, K V. Kabasura kudineer, a siddha medicine against COVID-19 infection: scope and future perspective. *Int J Complement Altern Med*. 2021;14(6):173—174. https://doi.org/10.15406/ijcam.2021.14.00554.
5. Kumar A, Rai A, Khan MS, et al. Role of herbal medicines in the management of patients with COVID-19: a systematic review and meta-analysis of randomized controlled trials. *J Tradit Complement Med*. 2022;12(1):100—113.
6. Divya M, Vijayakumar S, Chen J, Vaseeharan B, Durán-Lara EF. South Indian medicinal plants can combat deadly viruses along with COVID-19? - a review. *Microb Pathog*. 2020;148(12):104277. https://doi.org/10.1016/j.micpath.2020.104277.
7. Xu J, Zhang Y. Traditional Chinese medicine treatment of COVID-19. *Compl Ther Clin Pract*. 2020;39:101165. https://doi.org/10.1016/j.ctcp.2020.101165.
8. Khalifa I, Nawaz A, Sobhy R, Althawb SA, Barakat H. Polyacylated anthocyanins constructively network with catalytic dyad residues of 3CLpro of 2019-nCoV than monomeric anthocyanins: a structural-relationship activity study with 10 anthocyanins using in-silico approaches. *J Mol Graph Model*. 2020;100:1—11. https://doi.org/10.1016/j.jmgm.2020.107690.
9. Liu X, Wang XJ. Potential inhibitors against 2019-nCoV coronavirus M protease from clinically approved medicines. *J Genet Genomics*. 2020;47(2):119—121. https://doi.org/10.1016/j.jgg.2020.02.001.

10. Kirchdoerfer RN, Wang N, Pallesen J, et al. Erratum to: stabilized coronavirus spikes are resistant to conformational changes induced by receptor recognition or proteolysis. *Sci Rep.* 2018;8(1):15701. https://doi.org/10.1038/s41598-018-34171-7. Sci Rep. 2018;8(1):1–11. doi:10.1038/s41598-018-36918-8.

11. Song W, Gui M, Wang X, Xiang Y. Cryo-EM structure of the SARS coronavirus spike glycoprotein in complex with its host cell receptor ACE2. *PLoS Pathog.* 2018;14(8):e1007236. https://doi.org/10.1371/journal.ppat.1007236.

12. Burkard C, Verheije MH, Wicht O, et al. Coronavirus cell entry occurs through the endo-/lysosomal pathway in a proteolysis-dependent manner. *PLoS Pathog.* 2014;10(11):1–14. https://doi.org/10.1371/journal.ppat.1004502.

13. Li F. Structure, function, and evolution of coronavirus spike proteins. *Annu Rev Virol.* 2016;3(1):237–261. https://doi.org/10.1146/annurev-virology-110615-042301.

14. Duan L, Zheng Q, Zhang H, Niu Y, Lou Y, Wang H. The SARS-CoV-2 spike glycoprotein biosynthesis, structure, function, and antigenicity: implications for the design of spike-based vaccine immunogens. *Front Immunol.* 2020;11:1–12. https://doi.org/10.3389/fimmu.2020.576622.

15. Duquerroy S, Vigouroux A, Rottier PJM, Rey FA, Jan Bosch B. Central ions and lateral asparagine/glutamine zippers stabilize the post-fusion hairpin conformation of the SARS coronavirus spike glycoprotein. *Virology.* 2005;335(2):276–285. https://doi.org/10.1016/j.virol.2005.02.022.

16. Wang X, Xia S, Zhu Y, Lu L, Jiang S. Pan-coronavirus fusion inhibitors as the hope for today and tomorrow. *Protein Cell.* 2021;12(2):84–88. https://doi.org/10.1007/s13238-020-00806-7.

17. Xia S, Liu M, Wang C, et al. Inhibition of SARS-CoV-2 (previously 2019-nCoV) infection by a highly potent pan-coronavirus fusion inhibitor targeting its spike protein that harbors a high capacity to mediate membrane fusion. *Cell Res.* 2020;30(4):343–355. https://doi.org/10.1038/s41422-020-0305-x.

18. Shah B, Modi P, Sagar SR. In silico studies on therapeutic agents for COVID-19: drug repurposing approach. *Life Sci.* 2020;252:1–12. https://doi.org/10.1016/j.lfs.2020.117652.

19. Otvos RA, Still KBM, Somsen GW, Smit AB, Kool J. Drug discovery on natural products: from ion channels to nAChRs, from nature to libraries, from analytics to assays. *SLAS Discov.* 2019;24(3):362–385. https://doi.org/10.1177/2472555218822098.

20. Singh R, Bhardwaj VK, Sharma J, Purohit R, Kumar S. In-silico evaluation of bioactive compounds from tea as potential SARS-CoV-2 nonstructural protein 16 inhibitors. *J Tradit Complement Med.* 2022;12(1):35–43. https://doi.org/10.1016/j.jtcme.2021.05.005.

21. Bellik Y, Hammoudi S M, Abdellah F, Iguer-Ouada M, Boukraa L. Phytochemicals to prevent inflammation and allergy. *Recent Pat Inflamm Allergy Drug Discov.* 2012;6(2):147–158. https://doi.org/10.2174/187221312800166886.

22. Cornélio Favarin D, Martins Teixeira M, Lemos De Andrade E, et al. Anti-inflammatory effects of ellagic acid on acute lung injury induced by acid in mice. *Mediat Inflamm.* 2013;2013:1–13. https://doi.org/10.1155/2013/164202.

23. Government of India M of A. *GUIDELINES for SIDDHA PRACTITIONERS for COVID-19.* 2020. Published online.

24. Kannan M, Sathiyarajeswaran P, Sasikumar D, et al. Safety and efficacy of a siddha medicine fixed regimen for the treatment of asymptomatic and mild COVID-19 patients. *J Ayurveda Integr Med.* 2022:1–8. https://doi.org/10.1016/j.jaim.2022.100589. Published online.

25. Jose SP, M R, S S, et al. Anti-inflammatory effect of Kaba Sura Kudineer (AYUSH approved COVID-19 drug)-A Siddha poly-herbal formulation against lipopolysaccharide induced inflammatory response in RAW-264.7 macrophages cells. *J Ethnopharmacol.* 2022;283:1–7. https://doi.org/10.1016/j.jep.2021.114738.

26. Aljindan RY, Al-Subaie AM, Al-Ohali AI, Kamaraj B. Investigation of non-synonymous mutations in the spike protein of SARS-CoV-2 and its interaction with the ACE2 receptor by molecular docking and MM/GBSA approach. *Comput Biol Med.* 2021;135:104654. https://doi.org/10.1016/j.compbiomed.2021.104654.

27. Singh R, Bhardwaj VK, Purohit R. Inhibition of nonstructural protein 15 of SARS-CoV-2 by golden spice: a computational insight. *Cell Biochem Funct.* 2022. https://doi.org/10.1002/cbf.3753. Published online.

28. Singh R, Bhardwaj VK, Sharma J, Kumar D, Purohit R. Identification of potential plant bioactive as SARS-CoV-2 Spike protein and human ACE2 fusion inhibitors. *Comput Biol Med.* 2021;136:104631. https://doi.org/10.1016/j.compbiomed.2021.104631.

29. Xia S, Lan Q, Zhu Y, et al. Structural and functional basis for pan-CoV fusion inhibitors against SARS-CoV-2 and its variants with preclinical evaluation. *Signal Transduct Targeted Ther.* 2021;6(1):288. https://doi.org/10.1038/s41392-021-00712-2.

30. Shah BM, Modi P, Trivedi P. Pharmacophore- based virtual screening, 3D-QSAR, molecular docking approach for identification of potential dipeptidyl peptidase IV inhibitors. *J Biomol Struct Dyn.* 2021;39(6):2021–2043. https://doi.org/10.1080/07391102.2020.1750485.

31. Singh TU, Parida S, Lingaraju MC, Kesavan M, Kumar D, Singh RK. Drug repurposing approach to fight COVID-19. *Pharmacol Rep.* 2020;72(6):1479–1508. https://doi.org/10.1007/s43440-020-00155-6.

32. Huang H, Zhang G, Zhou Y, et al. Reverse screening methods to search for the protein targets of chemopreventive compounds. *Front Chem.* 2018;6:1–28. https://doi.org/10.3389/fchem.2018.00138.

33. Ounissi M, Rachedi FZ. Targeting the SARS-CoV-2 Main protease: in silico study contributed to exploring potential natural compounds as candidate inhibitors. *J Comput Biophys Chem.* 2022;21(6):663–682. https://doi.org/10.1142/s2737416522500272.

34. Halgren T. New method for fast and accurate binding-site identification and analysis. *Chem Biol Drug Des.* 2007;69(2):146–148. https://doi.org/10.1111/j.1747-0285.2007.00483.x.

35. Arya H, Bhatta TK. Molecular dynamics simulations. *Des Dev Nov Drugs Vaccines Princ Protoc.* 2021;12(2):65–81. https://doi.org/10.1016/B978-0-12-821471-8.00005-2.

36. Nutt DR, Smith JC. Molecular dynamics simulations of proteins: can the explicit water model be varied? *J Chem Theor Comput.* 2007;3(4):1550–1560. https://doi.org/10.1021/ct700053u.

37. Banks JL, Beard HS, Cao Y, et al. Integrated modeling program, applied chemical theory (IMPACT). *J Comput Chem.* 2005;26(16):1752–1780.

38. Mandal SK, Puri S, Kumar BK, et al. Targeting lipid-sensing nuclear receptors PPAR (α, γ, β/δ): HTVS and molecular docking/dynamics analysis of pharmacological ligands as potential pan-PPAR agonists. *Mol Divers.* 2023:0123456789. https://doi.org/10.1007/s11030-023-10666-y.

39. Valdés-Tresanco MS, Valdés-Tresanco ME, Valiente PA, gmx_Mmpbsa Moreno E. A new tool to perform end-state free energy calculations with GROMACS. *J Chem Theor Comput.* 2021;17(10):6281–6291. https://doi.org/10.1021/acs.jctc.1c00645.

40. Miller III BR, McGee Jr TD, Swails JM, Homeyer N, Gohlke H, Roitberg AE. MMPBSA. py: an efficient program for end-state free energy calculations. *J Chem Theor Comput.* 2012;8(9):3314–3321. https://doi.org/10.1021/ct300418h.

41. Shirts MR, Klein C, Swails JM, et al. Lessons learned from comparing molecular dynamics engines on the SAMPL5 dataset. *J Comput Aided Mol Des.* 2017;31:147–161. https://doi.org/10.1007/s10822-016-9977-1.

42. Ekberg V, Ryde U. On the use of interaction entropy and related methods to estimate binding entropies. *J Chem Theor Comput.* 2021;17(8):5379–5391. https://doi.org/10.1021/acs.jctc.1c00374.

43. Pires DEV, Blundell TL, Ascher DB. pkCSM: predicting small-molecule pharmacokinetic and toxicity properties using graph-based signatures. *J Med Chem.* 2015;58(9):4066–4072. https://doi.org/10.1021/acs.jmedchem.5b00104.

44. Delaney JS. ESOL: estimating aqueous solubility directly from molecular structure. *J Chem Inf Comput Sci.* 2004;44(3):1000–1005. https://doi.org/10.1021/ci034243x.

45. Malik AA, Phanus-umporn C, Schaduangrat N, Shoombuatong W, Isarankura-Na-Ayudhya C, Nantasenamat C. HCVpred: a web server for predicting the bioactivity of hepatitis C virus NS5B inhibitors. *J Comput Chem.* 2020;41(20):1820–1834. https://doi.org/10.1002/jcc.26223.

46. Shukla SS, Saraf S, Saraf S. Fundamental aspect and basic concept of siddha medicines. *Sys Rev Pharm.* 2011;2(1):48–54. https://doi.org/10.4103/0975-8453.83439.

47. Ms SD, P S, L K, K K, C S, Singh N. *In Vitro Antiviral Activity of Kabasura Kudineer - Siddha Polyherbal Formulation against Novel Coronavirus (SARS-CoV-2).* SSRN Electron J; 2021. https://doi.org/10.2139/ssrn.3842077. Published online.

48. Green DVS, Segall M. Chemoinformatics in lead optimization. *Chemoinformatics Drug Discov.* 2013:149–178. https://doi.org/10.1002/9781118742785.ch8. Published online.

49. Jain J, Narayanan V, Chaturvedi S, Pai S, Sunil S. In vivo evaluation of withania somnifera–based Indian traditional formulation (amukkara choornam), against chikungunya virus–induced morbidity and arthralgia. *J Evidence-Based Integr Med.* 2018;23:1–7. https://doi.org/10.1177/2156587218757661.

50. Wu H, Gong K, Qin Y, et al. In silico analysis of the potential mechanism of a preventive Chinese medicine formula on coronavirus disease 2019. *J Ethnopharmacol.* 2021;275:114098. https://doi.org/10.1016/j.jep.2021.114098.

51. Kiran G, Karthik L, Shree Devi MS, et al. In silico computational screening of kabasura kudineer - official siddha formulation and JACOM against SARS-CoV-2 spike protein. *J Ayurveda Integr Med.* 2022;13(1):1–8. https://doi.org/10.1016/j.jaim.2020.05.009.

52. Vincent S, Arokiyaraj S, Saravanan M, Dhanraj M. Molecular docking studies on the anti-viral effects of compounds from kabasura kudineer on SARS-CoV-2 3CLpro. *Front Mol Biosci.* 2020:434. https://doi.org/10.3389/fmolb.2020.613401. Published online.

53. Choudhary N, Singh V. Multi-scale mechanism of antiviral drug-alike phytoligands from Ayurveda in managing COVID-19 and associated metabolic comorbidities: insights from network pharmacology. *Mol Divers.* 2022:1–20. https://doi.org/10.1007/s11030-021-10352-x. Published online.

54. Manandhar S, Mehta CH, Nayak UY, Pai K. Structure-based docking, pharmacokinetic evaluation, and molecular dynamics-guided evaluation of traditional formulation against SARS-CoV-2 spike protein receptor bind domain and ACE2 receptor complex. *Chem Pap.* 2022;76(2):1063–1083. https://doi.org/10.1007/s11696-021-01917-z.

55. Di Petrillo A, Orrù G, Fais A, Fantini MC. Quercetin and its derivates as antiviral potentials: a comprehensive review. *Phyther Res.* 2022;36(1):266–278. https://doi.org/10.1002/ptr.7309.

56. Cheng HL, Zhang LJ, Liang YH, et al. Antiinflammatory and antioxidant flavonoids and phenols from Cardiospermum halicacabum (倒地鈴 Dào Dì Líng). *J Tradit Complement Med.* 2013;3(1):33–40. https://doi.org/10.1016/S2225-4110(16)30165-1.

57. Mandal SK, Kumar BK, Sharma PK, Murugesan S, Deepa PR. In silico and in vitro analysis of PPAR − α/γ dual agonists: comparative evaluation of potential phytochemicals with anti-obesity drug orlistat. *Comput Biol Med.* 2022;147:105796. https://doi.org/10.1016/j.compbiomed.2022.105796.

58. Govea-Salas M, Rivas-Estilla AM, Rodríguez-Herrera R, et al. Gallic acid decreases hepatitis C virus expression through its antioxidant capacity. *Exp Ther Med.* 2016;11(2):619—624. https://doi.org/10.3892/etm.2015.2923.

59. Mhatre S, Srivastava T, Naik S, Patravale V. Antiviral activity of green tea and black tea polyphenols in prophylaxis and treatment of COVID-19: a review. *Phytomedicine.* 2021;85:153286. https://doi.org/10.1016/j.phymed.2020.153286.

60. Wong TS, Tap FM, Hashim Z, et al. Dual actions of gallic acid and andrographolide trigger AdipoR1 to stimulate insulin secretion in a streptozotocin-induced diabetes rat model. *J Tradit Complement Med.* 2023;13(1):11—19. https://doi.org/10.1016/j.jtcme.2022.09.002.

61. Srivastava A, Rengaraju M, Srivastava S, et al. Efficacy of two siddha polyherbal decoctions, Nilavembu Kudineer and Kaba Sura Kudineer, along with standard allopathy treatment in the management of mild to moderate symptomatic COVID-19 patients—a double-blind, placebo-controlled, clinical trial. *Trials.* 2021;22(1):1—11. https://doi.org/10.1186/s13063-021-05478-0.